SPECIAL REPORT 95-2

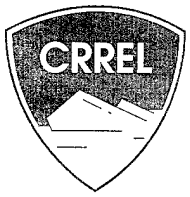

Winter Tests of Artillery Firing into Eagle River Flats, Fort Richardson, Alaska

Charles M. Collins and Darryl J. Calkins

January 1995

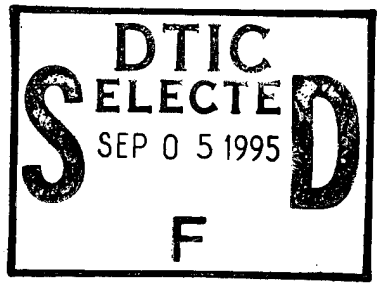

Abstract

Winter tests of artillery firing were conducted in the Eagle River Flats impact range to determine the physical effects of exploding high-explosive (HE) projectiles on the ice-covered terrain. Eagle River Flats is an estuary at the mouth of the Eagle River used as the artillery impact range for Ft. Richardson. The Army suspended use of the impact range following the discovery that white phosphorus (WP) deposited in the salt marsh was responsible for large numbers of waterfowl deaths each summer. The purpose of these tests was to assess if seasonal firing of HE projectiles from 60- and 81-mm mortars and 105-mm howitzers into Eagle River Flats could be resumed without significantly disturbing the sediments contaminated with WP. The results of the test firings indicated that a minimum of 25 cm of ice over frozen sediment or a minimum of 30 cm of floating ice over shallow water was required to prevent disturbance of the WP-contaminated sediment by exploding 105-mm howitzer projectiles. Only 10 cm of ice was required to prevent disturbance by exploding 60- and 81-mm mortar projectiles.

For conversion of SI metric units to U.S./British customary units of measurement consult ASTM Standard E380-89a, *Standard Practice for Use of the International System of Units,* published by the American Society for Testing and Materials, 1916 Race St., Philadelphia, Pa. 19103.

This report is printed on paper that contains a minimum of 50% recycled material.

Special Report 95-2

US Army Corps of Engineers
Cold Regions Research & Engineering Laboratory

Winter Tests of Artillery Firing into Eagle River Flats, Fort Richardson, Alaska

Charles M. Collins and Darryl J. Calkins

January 1995

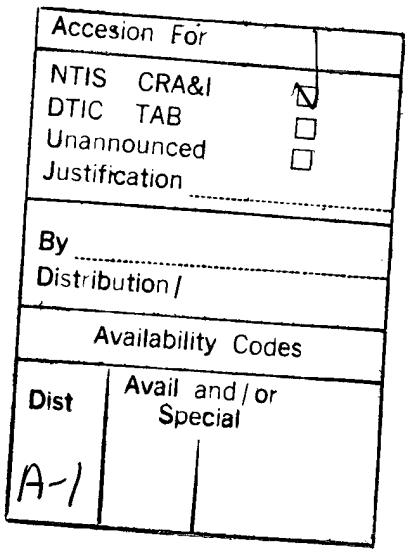

Prepared for
DIRECTORATE OF PUBLIC WORKS
FT. RICHARDSON, ALASKA

PREFACE

This report was prepared by Charles M. Collins, Research Physical Scientist, and Darryl J. Calkins, Chief, Geological Sciences Branch, Research Division, U.S. Army Cold Regions Research and Engineering Laboratory.

Funding for this effort was provided by the Directorate of Public Works, Sixth Infantry Division (Light), Ft. Richardson, Alaska.

The authors acknowledge William Gossweiler, Directorate of Public Works, Ft. Richardson, for his support in helping to arrange the test firing. The authors thank Bruce Brockett, Geological Sciences Branch, for his assistance in the field measurements of craters. The authors also thank Edward Chacho and Paul Sellmann for technically reviewing the manuscript. Finally, they thank the members of the 176th Explosive Ordnance Disposal Detachment for escorting them into the Eagle River Flats impact area and assisting them in the field measurements of craters.

CONTENTS

ILLUSTRATIONS

Figure

TABLES

Table

Winter Tests of Artillery Firing into Eagle River Flats, Fort Richardson, Alaska

CHARLES M. COLLINS AND DARRYL J. CALKINS

INTRODUCTION

The objective for the winter tests of artillery firing into the Eagle River Flats (ERF) impact area was to determine the physical effects of exploding rounds on winter terrain. The winter ground conditions of interest include snow cover, ice cover, frozen and unfrozen sediments and to some extent water beneath the ice covers in the pond areas. Observations were based on the disturbance of the snow, ice and sediment layers caused by exploding 105-, 81- and 60-mm high-explosive (HE) projectiles with both point detonation and delay fuses. To determine the effects of these projectiles, test firings using 105-mm howitzers and 60- and 81-mm mortars were conducted in a small portion of ERF during March 1991.

The purpose of these tests was to assess if seasonal firing of HE projectiles into ERF could be resumed without significantly disturbing contaminated sediments. Firing only during the winter, when the salt marsh is covered by a seasonal cover of snow, frozen ground and ice, might significantly reduce the disturbance of the sediments, compared to the previous practice of year-round firing.

BACKGROUND

Historical perspective

In 1990 white phosphorus (WP) was identified as the cause of waterfowl mortality in Eagle River Flats, a U.S. Army artillery impact range at Ft. Richardson, Alaska (Racine et al. 1992, 1993). Waterfowl use ERF as a resting, feeding and staging area during the spring and fall migration periods. In the past ten years, thousands of waterfowl have died annually in ERF. The WP particles found in the sediments of the shallow ponds were derived from WP smoke projectiles fired into the impact area over the years. The sediments are anoxic, allowing the particles of white phosphorus to persist for many years, posing a continual risk to waterfowl feeding in the ponds.

Firing into the impact area was suspended in February 1990. However, there is a continuing need to conduct artillery training at Ft. Richardson, and Eagle River Flats is the only feasible impact range available. Renewed artillery firing would only use high-explosive (HE) projectiles; the use of white phosphorus would be discontinued. Continued firing into ERF during the summer would cause redistribution and mixing of the bottom sediments in the shallow ponds and make buried WP particles accessible to feeding waterfowl. Winter firing into ERF has been proposed as a solution. The purpose of this study was to determine if the snow cover, ice cover and frozen ground that exist over extensive areas of ERF during the winter would isolate the sediments containing white phosphorus particles and prevent them from being disturbed or brought nearer to the surface by the explosion of artillery projectiles.

Environmental setting

Eagle River Flats, at the mouth of the Eagle River, is an 860-ha estuarine salt marsh on the south side of Knik Arm in upper Cook Inlet (Fig. 1). It is approximately triangular in shape, 2.75 km wide near the coast and 4 km long in an inland direction. It is bounded inland by a sharp topographic and vegetation boundary of spruce- and birch-covered uplands. The salt marsh is composed of a complex of landforms and vegetation zones. Natural levees occur along the banks of the river, with large expanses of sparsely vegetated mudflats along either side of the river and near the shore of Knik Arm. The backwater areas away from the river consist of zones of low sedge meadow, tall coarse sedge marsh and shallow open-water ponds (Racine

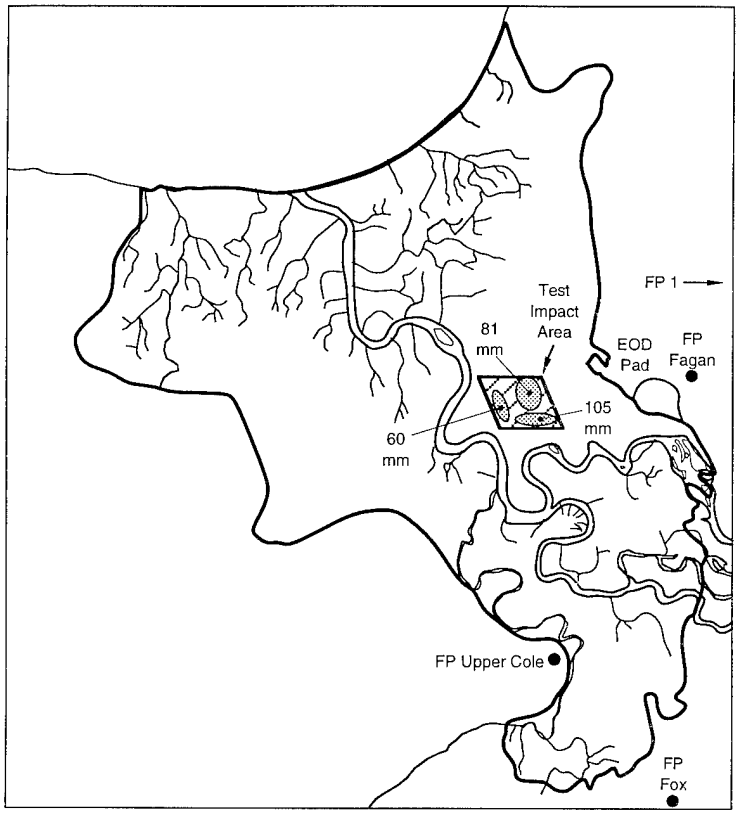

Figure 1. Eagle River Flats, showing the firing points and impact areas.

et al. 1993). The ponds, used by feeding waterfowl, are mainly located along the eastern and western perimeters of ERF. A 10-ha gravel pad (the EOD pad) is located along the eastern edge of ERF (Fig. 1). The EOD pad is a former open-burn, open-detonation disposal site.

Seasonally frozen ground

In areas of ERF without standing water, such as the mudflats, the natural levees and the tall coarse sedge marsh area adjacent to the EOD pad on the east side, the ground freezes each winter. The soils are generally saturated, and their properties generally do not vary appreciably. The soils consist of a mixture of silt and clay with a very small sand-size fraction (Racine et al. 1992). The depth of seasonal freezing primarily depends on the depth of the overlying snow cover, the frequency of tidal flooding and the seasonal air temperatures. Sediments underlying the shallow ponds along either side of the flats may or may not freeze, depending on the depth of the overlying water and whether the ice freezes completely to the bottom during the winter. In March 1991 the ground was frozen as deep as 40 cm in the tall coarse sedge marsh area adjacent to the EOD pad.

Ice cover conditions

The duration, extent and properties of the ice cover that forms over much of ERF during each winter are governed by meteorological conditions, snow cover, tidal effects, vegetation and local hydrology. The number and peak heights of high tides during the winter determine the extent of periodic inundations and the rate of ice buildup. Observations and measurements of the ice cover on a portion of ERF during the 1990-91 winter indicate a very complex situation (Taylor et al. 1994).

The extent and thickness of the ice cover are initially governed by the water surface elevations in the pond areas. The open ponds are normally the first areas to freeze over, forming congelation ice. Standing-water areas with heavy sedge and bulrush vegetation normally freeze later due to the insulating effect of the vegetation. Without tidal influences the growth of the ice sheet in the ponds will be a function of the heat loss (primarily radiation cooling and sensible heat conduction, both of which are affected by the snow cover thickness). A thin or nonexistent snow cover will promote rapid freezing; a thicker snow cover will reduce both radiative cooling and sensible heat conduction, thus reducing the rate of freezing. The weight of an even thicker snow cover, however, will exceed the buoyancy of the ice sheet, causing flooding of the sheet, saturation of the overlying snow cover and rapid ice thickening.

The role of the tides is important to both the continued growth of the existing ice sheets and extension of the area of ice cover. During a flooding high tide, water will back up in the channel of the Eagle River and then back up into the series of distributary channels and gullies that drain ERF into the Eagle River. The tide water floods out of the channels onto the mudflats and onto the ice-covered ponds; the water depth of the tide depends on the tidal elevation and the terrain features. When the water flows over an existing snow-free ice sheet or bare frozen ground when the air temperature is below freezing, a thin layer of ice is formed on the surface. This superimposed ice can

be built up in multiple layers by succeeding flooding tides.

The extent and thickness of the existing snow cover also play a role in the rate of ice buildup due to tidal flooding. When snow is present, the tidal water moves laterally through the snow cover and wicks upward several centimeters into the overlying snow pack, either partially or totally saturating the snow, depending on its thickness. Water under the snow that has only partially saturated the snow cover can remain unfrozen for a considerable length of time due to the insulating properties of the overlying snow. The saturated snow, when it freezes, produces a characteristic bubbly or white "snow ice" that is less dense than the clear congelation ice. This frozen saturated snow produces a thicker ice layer than would be produced if no snow cover had been present. Most high tides do not flood the entire flats. Rather, tidal flood water spreads out from the heads of tidal distributary channels as lobes or splays of water that saturate the snow cover, freeze and build up a layer of ice several centimeters thick over a limited area. These lobes of superimposed ice are then slightly higher than the surrounding non-flooded areas. Flooding water from the next high tide will then be displaced slightly, building up a lobe of ice adjacent to the previous ice lobes. Over time, much of the area of ERF can be covered by an ice sheet built up from successive multiple lobes of ice. An occasional extreme tide may flood the entire area, adding an additional ice layer.

During the 1990-91 winter, sparsely vegetated mudflat areas that are normally subaerially exposed in the summer had 30–60 cm of superimposed ice by March. The ice thickness in the ponds ranged from 40 to 70 cm, with the ice surface of the ponds as much as 20 cm above the normal summer water surface elevation due to the superimposed ice. In the mudflat areas where a superimposed ice sheet had formed, frozen sediments were found under the ice sheet, and in some cases the sediments were frozen greater than 40 cm. The brackish water from the tidal flooding did not appear to significantly alter the ice growth rate relative to freshwater behavior. The salinity gradient in ice samples ranged from brackish (20 ppt) near the river channel to fresh (<2 ppt) in the pond near the east edge of ERF. Petrographic and chemical analysis of the ice and sediment cores taken during the 1990-91 field season indicate a complex buildup of ice from tidal flooding and some freshwater runoff (Taylor et al. 1994).

The ice cover in the Eagle River within ERF continually moves up and down because of the tidal fluctuations. The surface of the ice sheet along the banks and extending into the channel was very smooth because of the constant flux of water from successive flooding. Ridges of broken ice, 2–4 m wide, in the centerline of the channel extend over a major portion of the river reach. Wide hinge cracks were evident along both shorelines at low tide. Ice chunks and flows up to several meters in diameter were scattered along either riverbank and extended a short distance from the channel. During the high tides, parts of the ice cover detached from the bank support, broke into small floes and floated onto the Flats for a short distance, depending on the terrain topography and water depth.

Impact area description

The impact area for the test was located on the east side of the Eagle River, about 500 m west of the EOD gravel pad, and covered an area of approximately 700 × 700 m (Fig. 1). Prior to the artillery tests, we characterized the site by measuring ice thicknesses and snow depths. Six ice cores were obtained using a hand-held 7.62-cm-diameter SIPRE core barrel. Ice thicknesses varied from 30 to 60 cm, with a minimum of 25 cm and a maximum of 40 cm of frozen sediment below the ice. The snow depth ranged from 15 to 20 cm within the test impact area, with an estimated snow density of 0.3 g cm^{-3}.

Previous research on cratering

Little information is available in the literature on the cratering and demolition effects of artillery fire on ice. A few 105- and 155-mm projectiles were fired onto the Imjin River in 1977 to determine their effectiveness in breaking floating ice covers; they were not effective. Several authors have looked at the effects of explosions in ice and snow (Livingston 1960, Mellor 1965), in frozen ground (Livingston 1956, 1959, Mellor and Sellmann 1970) and in and under floating ice sheets (Mellor 1982, 1986a, 1986b). Mellor (1986a) summarized the guidelines for blasting on ice sheets and gave estimates for the sizes of craters that will form, depending on the weight of the explosive charge and its position in the ice sheet.

The traditional analysis for determining the apparent scaled radius R_a and the scaled depth D_a of craters formed by explosions uses cube-root scaling (Mellor 1986a) to remove the effect of charge size (all linear dimensions are divided by the cube root

Table 1. Predicted apparent scaled radius and depth of craters.

	*Snow**	*Ice*†	*Frozen silt***
R_a	$0.87\ M_c^{1/3}$	$0.71\ M_c^{1/3}$	$0.56\ M_c^{1/3}$
D_a	$0.3–0.5\ M_c^{1/3}$	$0.24\ M_c^{1/3}$	$0.28\ M_c^{1/3}$

M_c is the mass of the explosive charge in kilograms.
Radius and depth of craters are in meters.
*Mellor (1965)
†Mellor (1986a)
**Mellor and Sellmann (1970)

of charge mass), allowing comparisons of craters formed by explosive charges of various sizes. For surface explosions, that is, explosions with a depth ratio of zero, the predictions in Table 1 can be made for the size of craters formed in snow, ice and frozen silt using the equations presented in Mellor (1965, 1986a) and Mellor and Sellmann (1970).

For example, a 105-mm howitzer M1 projectile, containing 2.3 kg of HE, has predicted apparent radii of the craters resulting from a contact burst for snow, ice and frozen silt of 1.15, 0.94 and 0.74 m, respectively. The predicted apparent depths would be 0.40–0.66, 0.32 and 0.37 m, respectively. The differences between the apparent crater formed by an explosion vs. the true crater may be substantial; they depend on whether the charge depth is zero (i.e. at the surface) or at some depth below the surface. The apparent crater is the excavation as it appears to an observer immediately after a blast (Livingston 1960). It often contains fall-back material, defined as the loose material thrown up by the explosion that has fallen back into the crater. Excavation of the fall-back material in the crater reveals the true crater.

ARTILLERY TESTS

The test firing onto the ice of Eagle River Flats took place on 20 March 1991. The test firing was conducted in three phases. The first phase consisted of firing a series of 105-mm howitzer HE projectiles with point-detonating fuses, the type of fuse and projectile normally fired into the ERF impact area for training. A series of HE projectiles with time-delay fuses was also fired to determine if the slight delay before detonation would allow the projectile to penetrate the ice cover before exploding. The HE projectiles were fired from M101A1 105-mm howitzers of the 4th Battalion, 11th Field Artillery. The howitzers were set up at Firing Point One (FP1), 4 km east of the impact area (Fig. 1). The second phase of tests used 81-mm mortar projectiles, using both point-detonating and delay fuses, into an area just north of the 105-mm impact area. The 81-mm mortars were set up at FP Fox, 1500 m southeast of the impact area. The third phase of tests consisted of 60-mm mortar projectiles with point-detonating fuses fired into an area west of the 105-mm impact area. The 60-mm mortars were set up at FP Upper Cole, 1000 m south of the impact area. The tests were observed and photgraphed from Observation Point Fagan, 1000 m east of the impact area. Firing information for the weapons used is presented in Table 2.

After the firing we photographed and measured the apparent diameters and apparent depths of the craters. Samples of snow were collected from around the craters to analyze for explosive residues.

All the dimensions given in this report are apparent crater diameters and depths. Because of the safety constraints and time limitations, none of the craters were excavated to measure true crater dimensions. However, except for the broken ice observed in the bottom of some 105-mm-howitzer craters, most craters appeared to have little loose material in them.

The analyses of our crater measurements assume that all explosions were contact bursts. A contact burst is one in which the center of mass of the exploding charge is at the surface, giving a depth ratio of zero. In actuality, the projectile with a point-detonating fuse may penetrate the surface by some unknown amount before exploding,

Table 2. Firing information for weapons used in the tests.

Weapon	*Round*	*Barrel angle*	*HE weight*
105-mm howitzer M101A1	105–mm HE M1	350–354 mils = 19.7–19.9°	2.3 kg (5.0 lb)
81-mm mortar M252	M374-A-3-81 mm	1217–1289 mils = 68.5–72.5°	0.95 kg (2.1 lb)
60-mm mortar M224	M49-A-4-60 mm	1166 mils = 65.6°	0.19 kg (0.42 lb)

because of the small time delay between the impact on the surface and the detonation of the explosion. In softer material such as mud or deep snow, where there is no hard surface to initiate the detonation, the point-detonating fuse will detonate once it senses a loss of momentum.

Based on the results of the March 1991 test, Eagle River Flats was reopened as an impact range in January 1992. Training began again in ERF on 7 January 1992, when the 4th Battalion, 11th Field Artillery fired a series of 105-mm howitzer projectiles into the impact range as part of a training exercise. Most projectiles impacted on the ice-covered levee and mudflats near the river. Several projectiles impacted on the ice-covered shallow ponds near the east side of the impact area. After the firing was completed we were able to measure several of the craters formed in the ice of the shallow ponds. We wanted to compare the effects of exploding 105-mm howitzer projectiles on a floating ice sheet with our previous observations on the effects on grounded ice and frozen ground. We also compared the measured crater parameters with the predicted parameters for explosives on floating ice.

Figure 2. Explosion of a 105-mm HE projectile in the test area.

RESULTS

105-mm howitzer test firing

Eight high-explosive 105-mm projectiles with point-detonating fuses were fired into the impact area. Seven of the eight projectiles detonated on contact with the ice (Fig. 2). The impact area had a 20-cm snow cover on the ice sheet, and the ice thickness varied from 0.30 to 0.60 m. The measurements of seven craters are included in Table 3 (craters no. 1–6 and 9); all values are for the apparent craters. All seven measured craters were oblong in shape, probably due to a low impact angle caused by the low firing angle (19.7–19.9°). The longest axis of the craters ranged from 2.26 to 3.63 m, and the shortest axis ranged from 1.89 to 3.05 m. The mean lengths for maximum and minimum axes were 3.17 and 2.45 m, respectively. This gives a mean apparent diameter of 2.81 m, or a mean apparent radius R_a of 1.41 m. The seven measured craters were shallow, between 0.2 and 0.44 m, with a mean apparent depth of 0.32 m. In all but one case, the ice sheet was still intact, with only a 0.6- to 1.0-m-diameter area of broken ice in the center of the crater (Fig. 3).

Figure 3. Crater formed by a 105-mm HE projectile.

Table 3. Measurement data from craters.

Crater no.	*Description*	*Maximum axis (m)*	*Minimum axis (m)*	*Center depth (m)*	*Snow depth (m)*	*Notes*
105-mm howitzer						
1	PD	2.26	1.89	0.30	0.20	
2	PD	2.90	2.10	0.44	0.20	1.2- × 0.6-m area of ground exposed at bottom of crater.
3	PD	3.29	2.50	0.37	0.20	
4	PD	3.38	2.32	0.39	0.20	
5	PD	3.20	2.77	0.30	0.20	
6	PD	3.63	2.50	0.27	0.20	0.6-m area in center where ice shattered.
7	D	1.07	0.61	—		Point where projectile ricocheted.
9	PD	3.54	3.05	0.20	0.20	0.6-m area of shattered ice in center.
8	D	7.62	2.44	0.20	0.20	Shallow, elongated crater. Ricocheted projectile blew up near surface.
10	D	3.00	2.40	0.35	0.20	
81-mm mortar						
1	PD	2.59	2.29	0.15	0.15	Bottom of crater is on top of ice sheet.
2	PD	2.49	2.29	0.16	0.15	
3	PD	2.26	1.86	0.16	0.15	
4	D	1.83	1.83	0.17	0.15	
5	D	Camouflet				Not measured.
6	D	Camouflet				0.6- × 2-m mound of ice rubble. 0.6-m-diam × approx. 1.8-m-deep crater hidden under rubble.
60-mm mortar						
1	PD	1.83	1.83	0.21	0.21	Depth of crater is equal to depth of snow on ice sheet, i.e. bottom of crater is top of ice sheet.
2	PD	1.83	1.52	0.15	0.15	
3	PD	1.80	1.89	0.18	0.18	0.10-m-diam × 0.08-m-deep hole in ice in exact center. Fuse parts in hole.
4	PD	1.83	1.52	0.22	0.20	
5	PD	1.83	1.83	0.17	0.17	

* PD = point-detonating fuse
D = delay fuse.

Figure 4. Ice lifted out of the bottom of crater no. 2, exposing frozen ground.

In one crater (no. 2 in Table 3), a 1.2- × 0.6-m area of the 0.25-m ice sheet was completely lifted and blown out of the crater, exposing the frozen ground underneath. The exposed frozen ground was not visibly disturbed or removed by the explosion (Fig. 4). There was no cratering of the frozen ground beneath the ice. One of the eight point-detonating projectiles was a dud, creating only a white plume of snow and ice when it hit the ice surface. The dud projectile produced a small crater estimated to be less than 1 m in diameter and of unknown depth; we did not measure this crater for safety reasons.

Figure 5. Ricocheting projectile exploding near the ice surface. The white plume of snow and ice shows where the projectile initially hit, and the explosion was just beyond it.

Four 105-mm projectiles with delay fuses were fired into the test area; three ricocheted off the ice before exploding, and one detonated in the snow and ice cover similar to the point-detonating projectiles. Figure 5 shows one ricocheting projectile exploding near the ice surface. This explosion produced a shallow elongated crater (no. 8) in the snow (Fig. 6), approximately 2.4 m wide at the near end, narrowing down to 0.6 m wide at the far end and 7.6 m long. Two ricocheting projectiles exploded in the air. Figure 7 shows the white plume of snow and ice where the projectile first hit and the dark explosion cloud high in the air (50 m?), near the skyline. The ricocheting projectile produced a small crater (no. 7), 1.07 × 0.60 m. The one delay-fused projectile that appeared to detonate normally produced a crater (no. 10) similar to those of the point-detonating fused projectiles, measuring 3.0 × 2.4 × 0.35 m.

All of these test firings of point-detonating and delay-fused 105-mm projectiles were done at a low angle of fire (19.7–19.9°). This is the standard procedure for firing into the impact range for training, with the projectiles reaching the target in the shortest time. A target can also be engaged from the same firing point with a high angle of fire, producing a high parabolic flight path, a longer flight time and a more vertical impact angle. Delay-fused 105-mm projectiles fired at a high angle would not

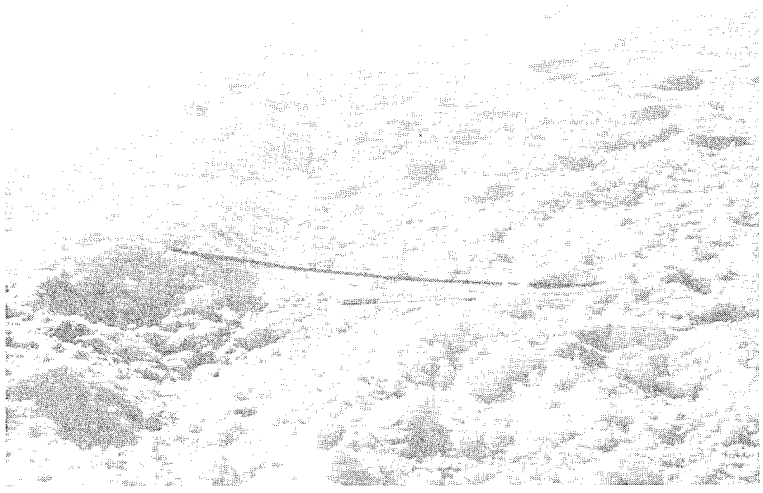

Figure 6. Shallow elongated crater produced by a ricocheting delay-fused projectile.

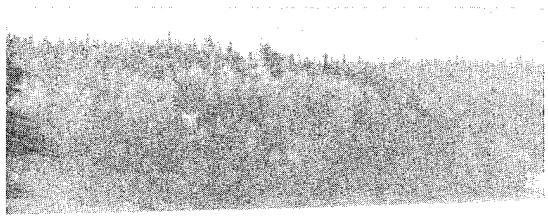

Figure 7. Ricocheting delay-fused projectile exploding high in the air.

be expected to ricochet but would penetrate the ice sheet before exploding, similar to the 81-mm delay-fused mortar projectiles discussed below.

81-mm mortar test firing

Both point-detonating and delay-fused 81-mm projectiles were fired during the test. Several of the mortar projectiles fell in the river and were inaccessible to us. We measured three craters formed by point-detonating projectiles. These craters averaged 2.45 × 2.15 m in diameter (Table 3), and they were more nearly circular than the howitzer craters, probably because of the higher trajectory of the mortar projectile. The mean apparent radius of the craters was 1.15 m.

The mean depth of the craters was 0.16 m, with most of the depth caused by removal of the 0.15-m-thick snow cover. A shallow depression was blown in the underlying ice cover in the center of the craters,

Figure 8. Crater formed by a point-detonating 81-mm mortar projectile on grounded ice.

Figure 9. Crater formed by a point-detonating 81-mm mortar projectile on a floating ice sheet.

but the ice was not broken or penetrated by the explosions (Fig. 8).

One of the point-detonating projectiles landed on the ice of a shallow pond north of the main impact area. The ice cover on the pond was 40 cm thick over about 30 cm of water. The crater (no. 1) produced by this projectile (Fig. 9) looked no different from the craters (no. 2 and 3) produced by projectiles landing on areas of grounded ice over frozen ground (Fig. 8).

Three delay-fused 81-mm projectiles (no. 4–6) landed in an area of grounded ice over frozen ground in the center of the test impact area. The cloud produced by the explosion of the 81-mm mortar projectiles was noticeably smaller than that produced by the 105-mm howitzer projectiles. The crater (no. 4) produced by the first projectile was similar to the 81-mm point-detonating projectiles but smaller and slightly deeper.

The second and third delay-fused projectiles each produced a camouflet, or a hidden crater. The projectiles penetrated the ice cover and the underlying frozen and unfrozen sediments before exploding. The confining strengths of the ice, the upper seasonally frozen sediment and the underlying saturated unfrozen sediment allowed the explosion to be confined and prevented it from ejecting material and producing a surface crater. The only evidence of the two camouflets was conical mounds of broken ice rubble, one of which measured 0.6 m high and 2 m in diameter (Fig. 10). Closer inspection and judicial digging into the mound by the EOD escort revealed a nearly vertical hole 30 cm in diameter and 1.5 m deep (Fig. 11).

Figure 10. Camouflet formed by a delay-fused 81-mm mortar projectile.

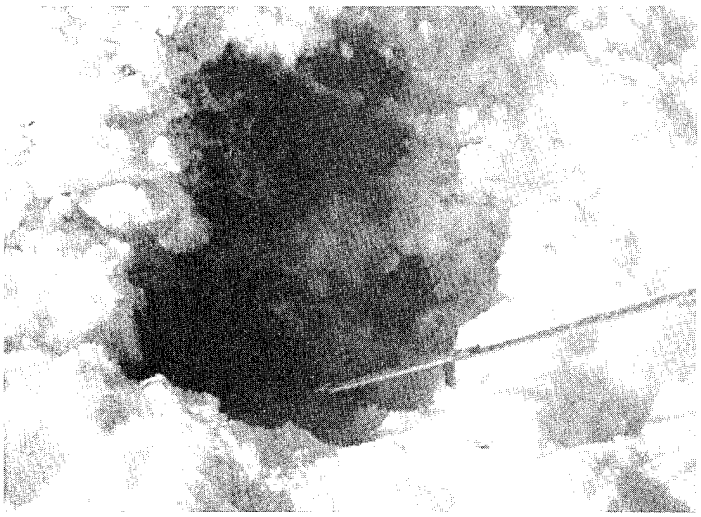

Figure 11. Nearly vertical hole in the camouflet.

60-mm mortar test firing

Only point-detonating 60-mm mortar projectiles were fired for the test. Craters produced by the 60-mm projectiles (Table 3, no. 1–5) were smaller than those produced by either the 105-mm howitzer or 81-mm mortar projectiles, averaging 1.83 × 1.70 m in diameter. This gives a mean apparent radius of 0.88 m.

The craters were very shallow, averaging 19 cm, essentially the depth of the snow cover in this part of the impact area. The snow was blown out by the explosion, and the underlying ice sheet remained intact (Fig. 12). There was usually a small dimple in the ice at the center of the crater where parts of the fuse of the projectile were sometimes found. One 60-mm projectile was a dud. The projectile appeared to penetrate into the ice (Fig. 13), with only the tail fins visible (again after careful digging of the snow around the projectile by the EOD escort).

Explosive residue

Snow around craters formed by 105-mm howitzer and 81-mm mortar projectiles was sampled and tested for the high-explosive components TNT and RDX. Darkened, ash-covered snow surrounding the crater was collected in a 500-mL I-Chem glass sample jar. The samples were returned to the laboratory and analyzed for HE components by high-performance liquid chromatography. No explosive components were detected, indicating that they were completely consumed in the explosions of the projectiles.*

January 1992 105-mm howitzer firing

Six craters formed in the ice sheet covering the shallow ponds along the eastern edge of the im-

* Personal communication with Marianne Walsh, CRREL, 1991.

Figure 12. Crater formed by a 60-mm mortar projectile.

Figure 13. Dud 60-mm projectile.

pact area were measured. The ponds in the area of impact are very shallow. The ice sheet covering the ponds was either partially grounded on the pond bottom or barely afloat. Because of the unevenness of the pond bottom sediment and the very soft nature of the sediment, it was difficult to determine the exact water depth beneath the ice cover. In part, the determination that an ice sheet was floating or not was based on the water surface level in the center crater. The water surface levels in four craters were obviously below the ice buoyancy point, indicating the ice sheet was grounded on the bottom at that location. The ice sheet at the other two crater locations was floating, although the water depths below the bottom of the ice sheet were only a few centimeters. The measured variables for these six craters are summarized in Table 4.

All the craters had a large, shallow outer crater formed in the overlying snow cover. All had a smaller inner crater consisting of a hole blasted through the underlying ice sheet. The longest axis of the outer craters ranged from 3.95 to 4.90 m, and the shortest axis ranged from 2.30 to 3.15 m. The mean lengths for maximum and minimum axes were 4.04 and 2.84 m, respectively. This gives a mean apparent diameter of 3.44 m, or a mean apparent radius R_a of 1.72 m. The depths of the outer crater averaged 0.17 m, which is the same as the average snow depth.

The longest axis of the inner crater or hole in the ice sheet ranged from 1.15 to 1.68 m, and the shortest axis ranged from 1.15 to 1.46 m. This gives a mean apparent diameter of 1.36 m, or a mean apparent radius R_a of 0.68 m. In the pond bottom sediments directly beneath the hole in the ice was a crater-shaped depression. However, at none of the craters was there any sediment displaced out of the hole and scattered on the surface. The shock wave of the explosion on the ice surface appeared to have compressed the soft pond bottom sediments into a crater-shaped depression without lifting or throwing sediment out of the hole. The center depth of the craters given in Table 4 is the total depth from the top of the original snow surface to the bottom of the depression in the pond bottom sediments. This averaged 0.68 m for the six craters.

ANALYSIS AND DISCUSSION

The analysis of the craters formed by the 105-m howitzers and 60- and 81-mm mortars and comparison of these crater data with published data on crater formation is complicated because these were formed by impacting projectiles, while much of the published data are for stationary explosive charges. Also, the published data are for a uniform medium, while these craters were formed in a three-layer medium with quite different densities and structural properties. The upper layer was snow, 0.15–0.19 m thick. The middle layer consisted of a 0.30- to 0.60-m-thick ice cover, and the bottom layer was a seasonally frozen, saturated fine-grained soil. The explosion of point-detonating mortar projectiles, both 60 and 81 mm, only removed the snow and rarely penetrated the surface of the ice cover. The explosion of point-detonating 105-mm howitzer projectiles removed the snow cover and at least part of the ice cover. In at least one case the entire ice cover was removed, but the crater did not penetrate into the underlying frozen soil layer.

105-mm howitzer test results

The mean apparent radius of the seven craters resulting from the point-detonating projectiles was 1.41 m. The mean scaled apparent radius of the

Table 4. Measurement data from craters on pond ice (105-mm howitzer).

Crater no.	*Max. axis (m)*	*Min. axis (m)*	*Max. axis in ice (m)*	*Min. axis in ice (m)*	*Center depth (m)*	*Snow depth (m)*	*Ice thick. (m)*	*Water depth in crater (m)*	*Water below ice sheet* (m)*	*Notes*
1	3.95	2.75	1.58	1.40	0.92	0.20	0.27	0.60	<0.01	ice partially grounded
2	4.90	3.05	1.20	1.20	0.50	0.14	0.25	0.29	<0.01	ice partially grounded
3	3.40	2.75	1.15	1.15	0.60	0.19	0.29	0.39	0.02	ice floating
4	3.95	3.05	1.43	1.37	0.63	0.16	0.22	0.40	<0.01	ice partially grounded
5	3.95	2.30	1.68	1.46	0.76	0.18	0.25	0.53	<0.01	ice partially grounded
6	4.10	3.15	1.43	1.22	0.66	0.16	0.25	0.48	0.03	ice floating
Ave.	4.04	2.84	1.41	1.30	0.68	0.17	0.26	0.45		

* The water depth below the bottom of the ice sheet is very difficult to measure because of the very soft pond bottom sediments.

seven craters was 1.07 m/kg$^{1/3}$. This is considerably larger than the predicted R_a of 0.71 m/kg$^{1/3}$ for ice and is out of the range of the scaled crater radius data for ice (Mellor 1986a). If we use the estimates for the scaled apparent radius of a crater in snow (Mellor 1965) instead of ice, we get closer agreement between the predicted and measured crater radii. The predicted value would be 0.87 m/kg$^{1/3}$ vs. the measured 1.07 m/kg$^{1/3}$.

The size of a crater created by an explosion increases as the depth of the explosive charge below the surface increases up to a certain depth, known as the critical depth. If we assume that the projectile did not explode at the surface but penetrated through the snow and a short distance into the ice (<0.05 m) before exploding, then the data would be within the maximum range of experimental data for ice presented by Mellor (1986a). However, there is no field evidence that the projectiles did penetrate into the ice before exploding.

The seven measured craters had a mean apparent depth of 0.32 m. This gives a scaled apparent depth of 0.25 m/kg$^{1/3}$, much shallower than the predicted depth for snow but almost the same as the predicted value given by Mellor (1986a) for ice. Obviously these comparisons are complicated by several factors. The experimental data used by Mellor in developing the scaled radius relationships were produced by static spherical explosive charges placed on the snow or ice surface. The artillery tests used a cylindrical projectile traveling at high velocity. The experimental data were for a single, uniform, semi-infinite-depth medium; we had a relatively thin, multiple-layered medium with quite different densities and structural properties.

The interaction of the snow and ice layer may explain the differences in crater size. As the 105-mm HE projectile penetrates the snow cover and the point-detonating fuse contacts the ice surface, the projectile explodes, producing a shock wave. The shock wave collapses the snow cover as it propagates downward and outward. Snow is a very good absorber of shock wave energy (Johnson et al. 1991, 1992), so the snow cushions part of the explosion. Part of the shock wave propagating downward will be reflected back off the snow–ice interface; this may increase the radius of the crater formed in the snow layer. Part of the shock wave will continue downward through the ice layer, hitting the ice–frozen soil interface. Part of the wave will then be reflected back up. This reflected wave, traveling back upward through the ice, can pop portions of the ice layer out of the crater without damaging the underlying frozen ground, as seen in one of the craters (Fig. 4). These reflected waves, traveling upward through the ice, may reduce or cancel later shock waves penetrating downward, thus reducing the total effect of the explosion.

81-mm mortar test results

The mean apparent radius of the three craters formed by point-detonating fused projectiles was 1.15 m, resulting in a scaled radius of 1.17 m/kg$^{1/3}$. The craters were almost entirely confined to the snow layer on top of the ice. The measured scaled radius is higher than the predicted scaled radius of a crater in snow from a surface-placed explosive.

The mean depth of the craters was 0.16 m, giving a scaled depth of 0.16 m/kg$^{1/3}$. Because the snow layer was shallow (0.15 m) and the crater was almost entirely confined to this layer, the scaled depth may be low because of the reflection of the shock wave off the ice layer, inhibiting the crater depth development.

60-mm mortar test results

Craters formed by the 60-mm mortar projectiles had a mean apparent radius of 0.88 m, or a scaled apparent radius of 1.53 m/kg$^{1/3}$. The craters were entirely confined to the snow layer. The measured scaled apparent radius was much higher than the predicted scaled radius of 0.87 m/kg$^{1/3}$. The measured scaled depth was 0.33 m/kg$^{1/3}$; this is very close to the predicted scaled depth for snow.

January 1992

105-mm howitzer firing results

The mean apparent radius of the outer craters formed in the snow on the ice sheet of shallow ponds was 1.72 m. The mean scaled apparent radius of the six craters was 1.30 m/kg$^{1/3}$. This is considerably larger than the predicted R_a of 0.87 m/kg$^{1/3}$ for snow, even larger than the differences noted in the March 1991 test firing. The mean apparent radius of the six inner craters or holes formed in the ice sheet of shallow ponds was 0.68 m. The mean scaled apparent radius of these inner craters is 0.90 m/kg$^{1/3}$, very close to the predicted scaled apparent radius of 0.94 m/kg$^{1/3}$ for ice.

The mean depth of the inner craters was 0.68 m, or a scaled depth of 0.52 m/kg$^{1/3}$. It is difficult to compare this to a predicted depth, since the inner crater completely pierced the ice sheet and extended into the soft pond bottom sediments below the ice.

CONCLUSIONS

The sizes of craters we measured during these tests were all larger than predicted from previous data for static spherical explosive charges set on the snow or ice surface. The mean scaled apparent radius of the craters formed by 105-mm point-detonating projectiles was 23% greater than predicted for a crater in snow and 50% greater than predicted for ice, 1.07 vs. 0.87 and 0.71 m/kg$^{1/3}$. The mean scaled apparent radius of the 81-mm point-detonating projectile craters was 1.17 m/kg$^{1/3}$, 34% larger than the predicted scaled apparent radius in snow and 65% larger than the predicted radius in ice. The 60-mm mortar projectiles produced craters confined to the shallow snow layer, with a mean scaled apparent radius of 1.53 m/kg$^{1/3}$, fully 76% larger than the predicted scaled radius in snow. The equations developed by Mellor (1986a) for predicting the scaled radius from experimental data greatly underestimate the radius of craters in layered snow and ice produced by artillery projectiles. On the other hand, the scaled depths of the artillery craters were similar to or less than the predicted depths; 0.25 vs. 0.4 and 0.24 m/kg$^{1/3}$ in snow and ice for the 105-mm projectiles, 0.16 vs. 0.4 and 0.24 m/kg$^{1/3}$ in snow and ice for the 81-mm mortars, and 0.33 vs. 0.40 m/kg$^{1/3}$ in snow for the 60-mm mortars.

The shapes of the craters formed were influenced by the multiple-layered medium of snow, ice and frozen ground into which the firing took place (Fig. 14). The greater-than-predicted radii of the craters

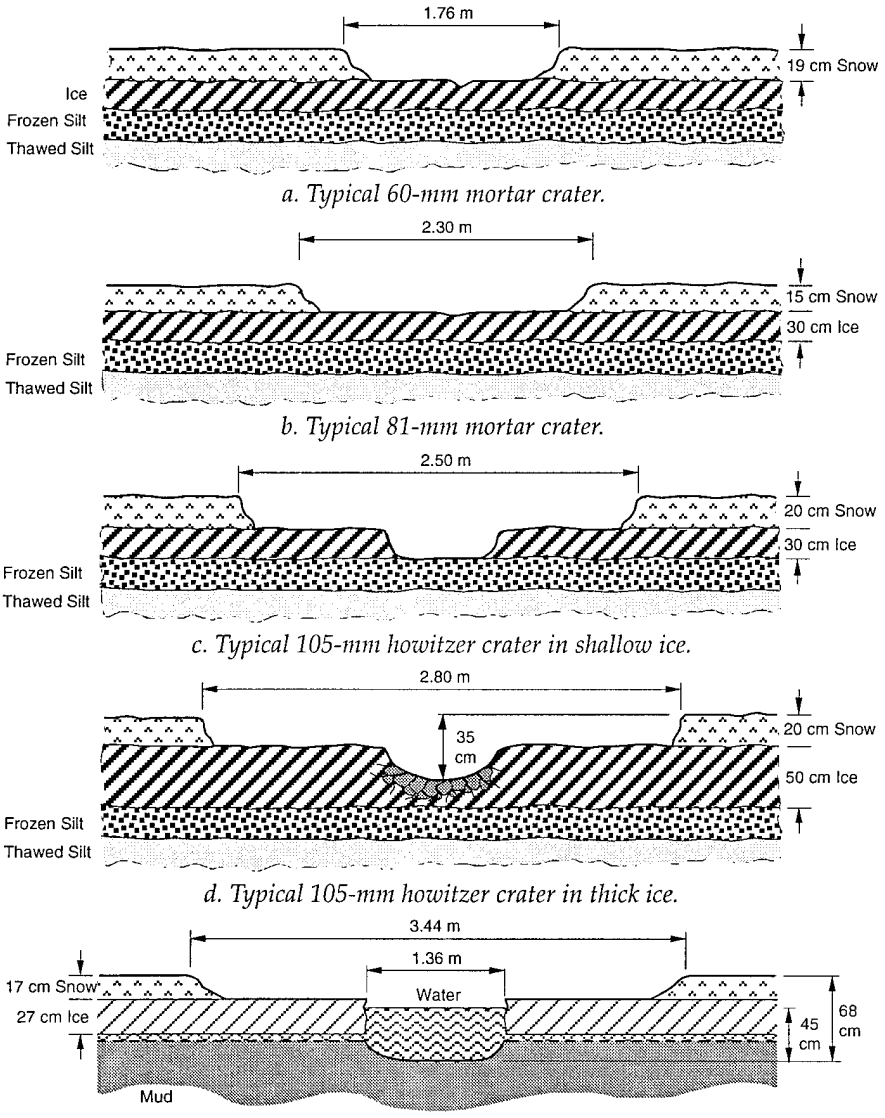

a. Typical 60-mm mortar crater.

b. Typical 81-mm mortar crater.

c. Typical 105-mm howitzer crater in shallow ice.

d. Typical 105-mm howitzer crater in thick ice.

e. Typical 105-mm howitzer crater in a floating ice sheet.

Figure 14. Typical crater cross sections.

can be attributed to the multiple-layered medium. The reflections of the shock waves off the multiple interfaces tended to decrease the depths of the craters, especially in the ice layer, and increase the radii of the craters in the snow layer.

In all cases the underlying frozen sediments were not disturbed when point-detonating projectiles were fired into Eagle River Flats with the ground frozen and covered with a 0.30- to 0.60-m ice sheet and 0.15- to 0.20-m of snow. The craters formed by point-detonating projectiles of both mortars and 105-mm howitzers were confined to the overlying snow and ice sheet. With the exceptions of one 105-mm and one 60-mm dud, all of the point-detonating projectiles performed satisfactorily. Delay-fused projectiles operated very erratically in areas with frozen ground and an ice cover.

The mean scaled apparent radius of craters we measured in January 1992 formed by 105-mm point-detonating projectiles in the ice sheet of shallow ponds were very close to those predicted from previous data for static spherical explosive charges set on the ice surface, 0.90 vs. 0.94 $m/kg^{1/3}$. However, the measured vs. scaled apparent radius of the outer crater in the shallow snow cover was 50% greater than predicted, again indicating the difficulty in predicting crater size in a shallow, multi-layered medium such as a thin snow layer over ice (Fig. 14).

In summary, based on the results of the test firing and observations of subsequent firing, winter firing into Eagle River Flats under conditions similar to those during the tests will not disturb the underlying sediments containing white phosphorus particles. For 105-mm howitzers, a minimum of 25 cm of ice over frozen sediment or a minimum of 30 cm of floating ice over shallow water is required. For 60- and 81-mm mortars, minimums are much less, on the order of 10 cm of ice. Winter firing with point-detonating projectiles when a sufficiently thick snow and ice cover is present appears to be the best approach to training in Eagle River Flats to prevent disturbance and mixing of the WP-contaminated sediments.

LITERATURE CITED

Johnson, J.B., J.A. Brown, E.S. Gaffney, G.L. Blaisdell and M. Sturm (1991) Shock wave studies of snow. In *Proceedings, Seventh Topical Conference on Shock Compression in Condensed Matter, Williamsburg, Virginia, 17–20 June 1991.* American Physical Society.

Johnson, J.B., J.A. Brown, E.S. Gaffney, G.L. Blaisdell and D.J. Solie (1992) Shock response of snow: Analysis of experimental method and constitutive model development. USA Cold Regions Research and Engineering Laboratory, CRREL Report 92-12.

Livingston, C.W. (1956) Excavations in frozen ground. Part I: Explosion tests in Keweenaw silt. USA Snow, Ice and Permafrost Research Establishment, Technical Report 30.

Livingston, C.W. (1959) Excavations in frozen ground. Part II: Explosion tests in frozen glacial till, Fort Churchill. USA Snow, Ice and Permafrost Research Establishment, Technical Report 30.

Livingston, C.W. (1960) Explosions in ice. USA Snow, Ice and Permafrost Research Establishment, Technical Report 75.

Mellor, M. (1965) Explosions and snow. USA Cold Regions Research and Engineering Laboratory, Monograph III A3a.

Mellor, M. (1982) Breaking ice with explosives. USA Cold Regions Research and Engineering Laboratory, CRREL Report 82-40.

Mellor, M. (1986a) Revised guidelines for blasting floating ice. USA Cold Regions Research and Engineering Laboratory, Special Report 86-10.

Mellor, M. (1986b) Blasting and blast effects in cold regions. Part II: Underwater explosions. USA Cold Regions Research and Engineering Laboratory, Special Report 86-16.

Mellor, M. and P.V. Sellmann (1970) Experimental blasting in frozen ground. USA Cold Regions Research and Engineering Laboratory, Special Report 153.

Racine, C.H., M.E. Walsh, C.M. Collins, D.J. Calkins and W.D. Roebuck (1992) Waterfowl mortality in Eagle River Flats, Alaska: The role of munition residues. USA Cold Regions Research and Engineering Laboratory, CRREL Report 92-5.

Racine, C.H., M.E. Walsh, C.M. Collins, S. Taylor, W.D. Roebuck, L. Reitsma and B. Steele (1993) White phosphorus contamination of salt marsh pond sediments at Eagle River Flats, Alaska. USA Cold Regions Research and Engineering Laboratory, CRREL Report 93-17.

Taylor, S., C.H. Racine, C.M. Collins and E. Gordon (1994) Ice formation in an estuarian salt marsh, Alaska. USA Cold Regions Research and Engineering Laboratory, Special Report 94-17.

REPORT DOCUMENTATION PAGE

Form Approved
OMB No. 0704-0188

1. AGENCY USE ONLY (Leave blank)	2. REPORT DATE	3. REPORT TYPE AND DATES COVERED
	January 1995	

4. TITLE AND SUBTITLE

Analysis of Artillery Winter Test Firing into Eagle River Flats, Fort Richardon, Alaska

5. FUNDING NUMBERS

6. AUTHORS

Charles M. Collins and Darryl J. Calkins

7. PERFORMING ORGANIZATION NAME(S) AND ADDRESS(ES)

U.S. Army Cold Regions Research and Engineering Laboratory
72 Lyme Road
Hanover, New Hampshire 03755-1290

8. PERFORMING ORGANIZATION REPORT NUMBER

Special Report 95-2

9. SPONSORING/MONITORING AGENCY NAME(S) AND ADDRESS(ES)

Directorate of Public Works
Sixth Infantry Division (Light)
Fort Richardson, Alaska

10. SPONSORING/MONITORING AGENCY REPORT NUMBER

11. SUPPLEMENTARY NOTES

12a. DISTRIBUTION/AVAILABILITY STATEMENT

Approved for public release; distribution is unlimited.

Available from NTIS, Springfield, Virginia 22161

12b. DISTRIBUTION CODE

13. ABSTRACT (*Maximum 200 words*)

Winter tests of artillery firing were conducted in the Eagle River Flats impact range to determine the physical effects of exploding high-explosive (HE) projectiles on the ice-covered terrain. Eagle River Flats is an estuary at the mouth of the Eagle River used as the artillery impact range for Ft. Richardson. The Army suspended use of the impact range following the discovery that white phosphorus (WP) deposited in the salt marsh was responsible for large numbers of waterfowl deaths each summer. The purpose of these tests was to assess if seasonal firing of HE projectiles from 60- and 81-mm mortars and 105-mm howitzers into Eagle River Flats could be resumed without significantly disturbing the sediments contaminated with WP. The results of the test firings indicated that a minimum of 25 cm of ice over frozen sediment or a minimum of 30 cm of floating ice over shallow water was required to prevent disturbance of the WP-contaminated sediment by exploding 105-mm howitzer projectiles. Only 10 cm of ice was required to prevent disturbance by exploding 60- and 81-mm mortar projectiles.

14. SUBJECT TERMS

Artillery
Eagle River Flats
High-explosive projectiles
Ice-covered terrain

15. NUMBER OF PAGES
21

16. PRICE CODE

17. SECURITY CLASSIFICATION OF REPORT	18. SECURITY CLASSIFICATION OF THIS PAGE	19. SECURITY CLASSIFICATION OF ABSTRACT	20. LIMITATION OF ABSTRACT
UNCLASSIFIED	UNCLASSIFIED	UNCLASSIFIED	UL

NSN 7540-01-280-5500

☆U.S. GOVERNMENT PRINTING OFFICE: 1995-0-600-856

Standard Form 298 (Rev. 2-89)
Prescribed by ANSI Std. Z39-18
298-102